Evidence for short-range correlations from high Q^2 (e, e') reactions

L. L. Frankfurt
Department of Physics, Tel Aviv University, Ramat Aviv, 69978 Tel Aviv, Israel

M. I. Strikman
Department of Physics, Pennsylvania State University, State College, Pennsylvania 16802

D. B. Day
Institute of Nuclear and Particle Physics, University of Virginia, Charlottesville, Virginia 22901

M. Sargsyan
Yerevan Physical Institute, Yerevan, Armenia
(Received 20 April 1992)

We argue that the ratio of cross sections of quasielastic electron scattering for heavy and light nuclei at $x > 1$ and $Q^2 > 1$ $(\mathrm{GeV}/c)^2$ should exhibit simple scaling relations which are ultimately expressed through the ratio of the light-cone nucleon distributions in nuclei. We extract these cross section ratios from existing data in a practically model independent way. The results are found to be in reasonable agreement with our x-scaling relations for the region of $2 > x \geq 1.4$ where the contribution of two-nucleon short-range correlations are expected to dominate. The ratios exhibit scaling in the light-cone fraction, α, of the struck nucleon for the range $2 > x \geq 0.9$. The α scaling is in agreement with the expectations of the light-cone quantum mechanics of nuclei, providing further evidence for the dominance of short-range correlations in nuclei at $k > 0.3$ GeV/c. An extension of this analysis to the interpretation of color transparency experiments is discussed.

PACS number(s): 25.30.Fj

I. INTRODUCTION

For many years now short-range correlations (SRC) in nuclei have been considered as an essential feature of the nuclear wave function. However, at medium energies the influence of SRC is hidden by the effects of multistep processes dominated by the soft (low momentum) components of the wave function. The situation improves significantly at high energies which allow one to select processes in which (a) the scattering from low momentum nucleons is kinematically suppressed and (b) the energy transfer exceeds the characteristic kinetic energies of correlated nucleons in the nucleus.

One of the simplest reactions which satisfies both these requirements is $A(e, e')$ at

$$Q^2 > 1\,(\mathrm{GeV}/c)^2 \text{ and } x = \frac{Q^2}{2mq_0} > 1, \qquad 1\,\mathrm{GeV} > q_0 > 300 \sim 400\,\mathrm{MeV}, \tag{1}$$

where $m = m_N$ and q_0 is the energy transfer. These reactions have been intensively investigated during the last decade or so at SLAC on both light and heavy nuclei [1–5]. In this paper we argue for the existence of simple scaling relations between the cross sections of light and heavy nuclei in the kinematics where electron scattering off SRC should dominate. We present ratios extracted from data which demonstrate that these relations are reasonably well satisfied and which emphasize the dominance of two-nucleon SRC in the spectral function for $k > 0.3$ GeV/c.

This paper is organized as follows. In Sec. II we explain the specifics of the space-time evolution of the final states in the $A(e, e')$ reactions in the kinematics given by Eq. (1), which helps us account for the final state interaction (fsi). In Sec. III we use the nonrelativistic impulse approximation to deduce the scaling relations between cross sections of the $A(e, e')$ reaction on different nuclei. Therein we explain how, within our model, the fsi cancels in the ratios of the cross sections, though it contributes to the individual cross sections. In Sec. IV we describe the procedure we developed for extracting the ratios from existing experimental data and demonstrate that the extracted ratios agree with the scaling relations. In Sec. V we explain why and how relativistic kinematics leads to the light-cone dynamics of the process. We generalize the scaling relations for relativistic kinematics and calculate the ratios of the cross sections in terms of the light-cone quantum mechanics of nuclei. We also explain in Sec. V how the extracted ratios could be used to improve analyses of $A(e, e'p)$ experiments at large Q^2 undertaken to investigate color transparency phenomena. In the Appendix we discuss the fsi of the struck nucleon with the slow nucleons of the nucleus.

The physics of quasielastic processes [which dominates the cross section in the kinematics of Eq. (1)] has been discussed in detail in the analyses [6,7], so that here we only outline the ideas leading to basic formulas.

II. SPECIFICS OF SPACE-TIME EVOLUTION OF FINAL STATE INTERACTION AND APPROXIMATIONS

The kinematics of Eq. (1) allows one to compute the cross section through processes local in space if

$$q_0 = \frac{Q^2}{2mx} \text{ and } |\mathbf{q}| = q_3 = \sqrt{Q^2 + Q^4/4m^2x^2} \qquad (2)$$

are sufficiently large. To explain this, let us analyze the representation of the cross section as a Fourier transform of the commutator of electromagnetic currents:

$$2m_A q_3 \sigma^{(r)} = \int e^{iqy} \langle A \mid [j_\mu(y), j_\lambda(0)] \mid A \rangle \epsilon_\mu^{(r)} \epsilon_\lambda^{(r)} d^4y. \qquad (3)$$

Here $\epsilon^{(r)}$ is the polarization vector of the virtual photon. For the kinematic region of interest, where the contribution of inelastic processes is suppressed by phase space, it is appropriate to consider the ratio $\tilde{\sigma} = \sigma/G^2(Q^2)$, where $G^2(Q^2)$ is the square of the nucleon electromagnetic form factor. Equation (3) is also valid for $\tilde{\sigma}$; we then use $\tilde{j}_\mu$, the electromagnetic current for photon interaction with a pointlike nucleon.

Introducing the light-cone (LC) coordinates $y_\pm = y_0 \pm y_3$ we see that in the domain given by Eq. (1), where $q_\pm = q_0 \pm q_3$ are large on the scale characteristic for nuclear phenomena, the major contribution to Eq. (3) is given by the region of integration where

$$y_+ \sim \frac{1}{q_-} < 1\,\text{fm}, \; y_- \sim \frac{1}{q_+} < 0.2\,\text{fm}. \qquad (4)$$

(We use the system of units where the velocity of light is equal to 1.) Using the causality condition, $[j_\mu(y), j_\lambda(0)] = 0$, for $y^2 < 0$ implies that

$$y^2 = y_+ y_- - y_t^2 > 0, \qquad (5)$$

leading to

$$y_t^2 < \frac{1}{Q^2}. \qquad (6)$$

This estimate of the Fourier transform is based on the oscillatory behavior of the exponent in Eq. (3), the causality condition, and the presence of singularities in the amplitudes at small space-time timelike intervals. A simple method to numerically check this estimate is to reconstruct, from the experimental data, the matrix element of the commutator of electromagnetic currents (cf. [7]). Therefore the significant fsi of the struck nucleon would occur only with nucleons which are very close to it. We give additional arguments in favor of this conclusion in the Appendix.

It is easy to check that for our particular kinematics, the struck nucleon and its nearest neighbors in the initial state have large and comparable momenta in the final state, while the rest of the nucleons, which were at large distances from the struck nucleon in the initial state, end up with small momenta [6,7]. Therefore the fsi of the struck nucleon and fast spectators with slow ones can be calculated using the usual semiclassical approximation for the interaction of fast particles with slow ones. If the energy transferred to the struck nucleon significantly exceeds the characteristic kinetic energies of the nucleons in nuclei ($\sim$ 40 MeV) this fsi can be well accounted for within the semiclassical approximation by closure. The validity of the completeness approximation can be checked within the optical model description for the interaction of the fast ejected nucleons with the rest of the nucleons. However, it is not legitimate to apply the semiclassical approximation to the interaction of a struck nucleon with the nucleon which has comparable momentum in the final state, since in this case the invariant energy of the two-nucleon interaction is not large—the relative momenta of these nucleons in their center-of-mass (c.m.) frame are $k_1 = -k_2 = \sqrt{\frac{Q^2(2-x)}{4x}}$. Remember that this nucleon has been the neighbor of the struck nucleon in the initial state [6,7] (see also Sec. III). In particular, for the kinematics set by Eq. (1), the fsi between the struck nucleon and its neighbors increases the cross section by as much as 50% as calculated for the deuteron [8]. Thus, we conclude that the fsi's are not small but are nearly local in space. The interaction of the struck nucleon with the slow spectator nucleons of nuclei may reveal itself in $(e, e'p)$ reactions where the closure (completeness) approximation discussed above is inapplicable. It will be important to calculate any differences in the fsi's (presumably quite small) due to the motion of the pair in the mean field of nucleus by which the final state mass of the pair deviates from that of the deuteron.

III. NONRELATIVISTIC IMPULSE APPROXIMATION

In virtual photon-nucleon scattering, energy-momentum conservation laws restrict x to be less than unity if the target nucleon is at rest. The kinematic boundary $x = 1$ corresponds to elastic e-p scattering. This well known result can be easily generalized for e-A scattering in the impulse approximation. A similar consideration of the kinematics of nucleons in the final state shows that for $x > j - 1$ momenta of j nucleons should be *large* at large Q^2 [6,7]. Hence the j nucleons are close to each other and the influence of the other $(A-j)$ nucleons on their wave function is small, provided the nearest-neighbor (NN) interaction is sufficiently singular at small r_{NN}. Numerical calculations of the nucleon density of nuclei in momentum space show that its shape becomes essentially independent of atomic number for nucleon momenta $k > 0.4$ GeV [9].

To convey the basic ideas, we start with the nonrelativistic impulse approximation as a guide. The generalization to include relativistic kinematics and fsi is presented below. Nuclear wave functions contain mean-field and correlation effects, with the high momentum nucleons arising from the effects of correlations. Thus nonrelativistic spectral functions containing one nucleon with large momentum can be represented as the sum which in-

cludes contributions of few (2,3, ...) nucleon correlations. This approximate description agrees reasonably well with current numerical calculations of spectral functions of the lightest nuclei and of infinite nuclear matter, where two-nucleon correlations are dominant, provided the center of mass motion of the pair is taken into account. (See the discussion in Ref. [10].) The same decomposition over the contributions of few nucleon correlations is valid for the scattering from more exotic compact configurations in nuclei discussed in the literature, e.g., ΔN, 6-quarks, etc. In line with the experimental evidence that the contribution of meson currents to the cross section of hard processes is small [13], we systematically neglect in this work the possible effects of meson currents.

By considering that in the kinematics of Eq. (1) nucleon-nucleon correlations should dominate, we can approximate the inclusive cross section in the following way:

$$\sigma(x,Q^2) = \sum_{j=2}^{A} A\frac{1}{j} a_j(A)\sigma_j(x,Q^2) \ , \qquad (7)$$

where $\sigma_j(x,Q^2) = 0$ at $x > j$ and $a_j(A)$'s are proportional to the probabilities to find a nucleon in a j-nucleon correlation. The mathematical observation that the high momentum behavior of Fourier transforms of the wave function is determined by singularities of the potential should be recalled here. Therefore the high momentum behavior of the contribution of SRC to the spectral function is universal and does not depend on A. This is the essential assumption required for the Jastrow correlations to describe nuclei. At this point, we ignore the different functional dependence for the contributions of correlations with different isospin and spin. In any case, for pair-nucleon correlations the contribution of nucleon pairs with isospin 0 dominates due to combinatorics [11]. We choose σ_2 to be equal to the electron-deuteron cross section to define the normalization, and then a_2 is closely related with the number of quasideuteron pairs in the nucleus. Similarly, σ_3 is the cross section for the scattering from ^{3}He. Thus Eq. (7) is a reasonable interpolating formula. It accounts for the fact that in the region $j > x > j-1$ the contribution of j-nucleon SRC dominates. It should, however, be pointed out that the parametrization given by Eq. (7) implies that the center of mass of the j-nucleon cluster is at rest; the validity of such an approximation has to be investigated, since it was shown in [10] that the center-of-mass motion plays a role in determining the removal energy dependence of the spectral function.

Since the nucleus is a rather dilute system, in any realistic model a_j should rapidly decrease with j. Therefore, Eq. (7) leads to the following scaling relations between scattering off the lightest nuclei ($A = 2$) and heavier nuclei (these relations were suggested in [6] within the few nucleon correlation model and implicitly in [12] for the scattering off ^{3}He within the quark cluster model):[1]

$$\frac{2}{A}\frac{\sigma_A(x,Q^2)}{\sigma_D(x,Q^2)} = a_2(A)|_{1<x\leq 2}$$

and (8)

$$\frac{3}{A}\frac{\sigma_A(x,Q^2)}{\sigma_{A=3}(x,Q^2)} = a_3(A)\ |_{2<x\leq 3} \ .$$

The dominance of the contribution of pair nucleon correlation in the $x < 2$ region was also suggested in [14]. We have chosen the scale of σ_j so that $\sigma_D(x,Q^2) = \sigma_2(x,Q^2)$, etc.

The evident advantage of Eq. (8) is that in the impulse approximation the cross section for the virtual gamma scattering off a nucleon is canceled in the ratio as are any off-shell effects in the interaction of the virtual photon with the struck nucleon. The fsi between the outgoing nucleons of the SRC is proportional to the internucleon wave function at small distances and therefore weakly depends on the nuclear environment. As a result this fsi is canceled out in the cross section ratios if the motion of the pair in the mean field is neglected. This property of the wave functions of the final state is an analogue of the above mentioned independence of the Jastrow correlations on the nuclear environment. In particular, we may safely ignore possible differences between fsi for different channels for $1 < x < 2$. Corrections to Eq. (8) arise due to the difference of the fsi for $I = 0$ and $I = 1$ outgoing NN systems. However this difference is small enough if $M_{NN} - 2M_N > 50$ MeV, as it is in the kinematics we study below. Additionally, the scattering of the $I = 0$ pairs contributes greater than 80% of the cross section [11].

IV. SCALING RELATIONS AND EXPERIMENTAL DATA

There exists a considerable body of data from the deuteron and heavier nuclei which cover the (x,Q^2) range of interest here. As no single experiment includes both the deuteron and heavy nuclei, the data sets, taken at various incident and final energies and electron scattering angles, are not at the same values of (x,Q^2) necessary to form the ratios in Eq. (8). The data sets, however, span a common region in the (x,Q^2) plane such to make it possible to form the ratios in a straightforward way which we now describe.

The inclusive experimental cross sections at large Q^2 for all nuclei are a smooth function of x, falling steeply at large x. The original bin sizes of the data used here are quite small, with energy loss bins of typically no larger than 15 MeV. In order to improve the available statistics and to provide common x bins we rebinned data for all nuclei into less than two dozen x bins spanning $0.8 < x < 2$, with the largest x bin centered at 1.9. After the inclusive cross sections were rebinned, it was necessary to take into account the different Q^2, which were unique for every x bin. We selected the experiment on

[1] It is trivial to generalize Eqs. (7) and (8) to take into account the isospin dependence of SRC.

heavy nuclei [5] to define the kinematics of the ratios given below (since in that experiment data on ^{4}He, C, Al, Fe, and Au were obtained at identical energies and angles). To form the ratios it was then necessary to fit at each x the Q^2 dependence of the deuteron data and to evaluate the fit at the Q^2 of the heavy nucleus. Most of the deuteron Q^2 dependence is due to the elastic form factor of the the nucleon and can be accounted for by an impulse model calculation of the cross section. This is a good approximation, since the fsi's change only slightly over the small Q^2 interval involved in the interpolation. We removed this Q^2 dependence before making the fit using the y-scaling model [5]; after the fit was evaluated at the appropriate (x, Q^2) the resultant was renormalized with the same model. We required that for every x point at least three spectra contribute to the fit. For all nuclei at the lowest $Q^2 \sim 0.9$ GeV/c^2 for $x < 1.25$, we evaluated the fit of the Q^2 dependence outside the kinematic boundary defined by the deuteron data. This contributes only slightly to the error as the fit was strongly determined by a nearby [at $Q^2 \approx 1.2$ (GeV/c)^2] data set with small error bars. For Fe, for the two highest Q^2 spectra, we similarly extended the fit for the x range between 1.4 and 1.5 with an estimated contribution of 5% to the error.

All the data we have used were obtained at SLAC. The deuteron data are from [15,1,2] and the heavy nuclei from [5]. Data from ^{3}He are from [4,16]. We show in Figs. 1–4 the ratios of $\frac{2}{A}\frac{\sigma^A(x,Q^2)}{\sigma^D(x,Q^2)}$ for ^{4}He, ^{27}Al, ^{56}Fe, and ^{197}Au at four (six for Fe) values of Q^2. For nuclei not shown (^{3}He and C) the ratios have identical characteristics. One can see that Eq. (8) is satisfied within experimental errors in the kinematics where, according to our model calculations, two-nucleon correlations should dominate. At these x ($x > 1.3 - 1.4$) $a_2(A)$ does not depend on x and Q^2. If we average a_2 over all $\alpha_{tn} \geq 1.25$ (α_{tn} is introduced below and the range we have averaged over corresponds approximately to values of $x \geq 1.4$), we find

$$
\begin{aligned}
a_2(^3\mathrm{He}) &= 1.7(0.3)\ , \\
a_2(^4\mathrm{He}) &= 3.3(0.5)\ , \\
a_2(^{12}\mathrm{C}) &= 5.0(0.5)\ , \\
a_2(^{27}\mathrm{Al}) &= 5.3(0.6)\ , \\
a_2(^{56}\mathrm{Fe}) &= 5.2(0.9)\ , \\
a_2(^{197}\mathrm{Au}) &= 4.8(0.7)\ ,
\end{aligned}
$$

where the number in parentheses is the standard deviation. The average value is much larger than the standard deviation, suggesting the independence of a_2 on x and Q^2. Data with better statistics will be necessary to look for any possible deviations from a Q^2 independent $a_2(A)$. The interpretation of these ratios may be difficult for kinematics very close to threshold for disintegration. We have therefore indicated in Figs. 1–4 those values of x that result from scattering to a final hadronic state which exceeds the deuteron mass by less than 50 MeV. Note that in these kinematics the light-cone dynamics

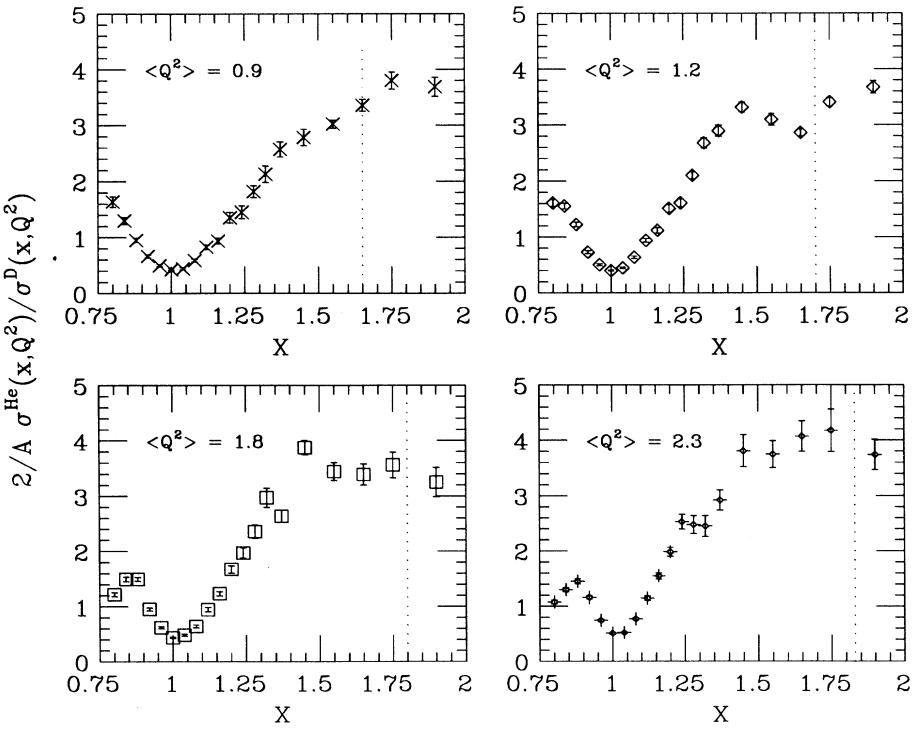

FIG. 1. Ratio $\frac{2}{A}\frac{\sigma_A(x,Q^2)}{\sigma_D(x,Q^2)}$ for ^{4}He at four different Q^2's. The average Q^2 is given for each frame. To the right of the vertical dashed line are those data which correspond to a final state less 50 MeV greater than the deuteron rest mass.

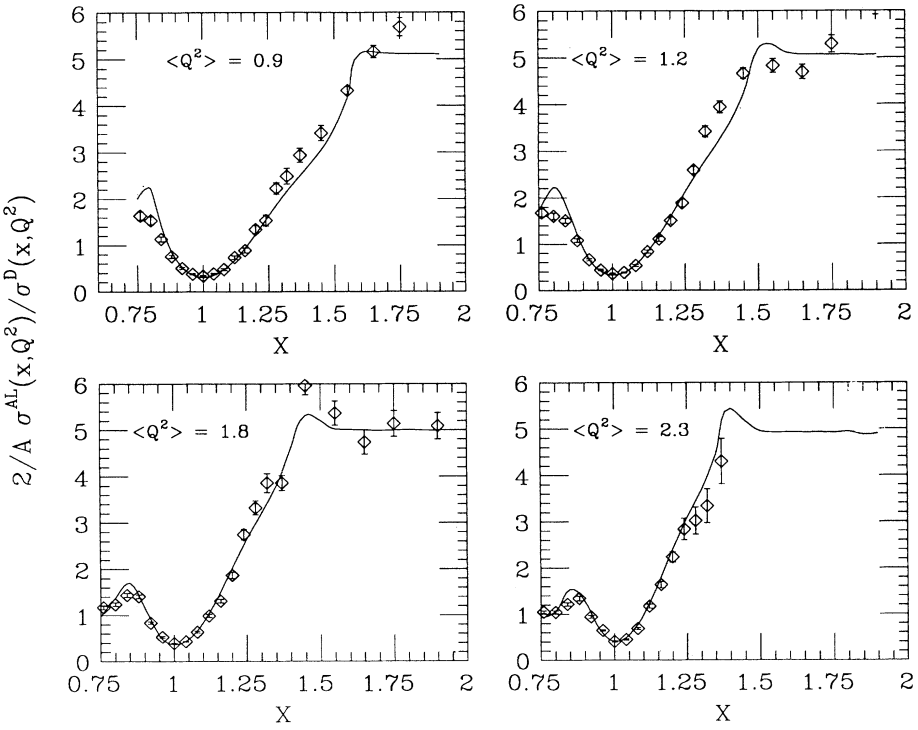

FIG. 2. Ratio $\frac{2}{A}\frac{\sigma_A(x,Q^2)}{\sigma_D(x,Q^2)}$ for ^{27}Al at four different Q^2's. The average Q^2 is given for each frame. To the right of the vertical dashed line are those data which correspond to a final state less 50 MeV greater than the deuteron rest mass. The solid line is a calculation based on the nuclear spectral function of Ref. [22] (see Sec. VI).

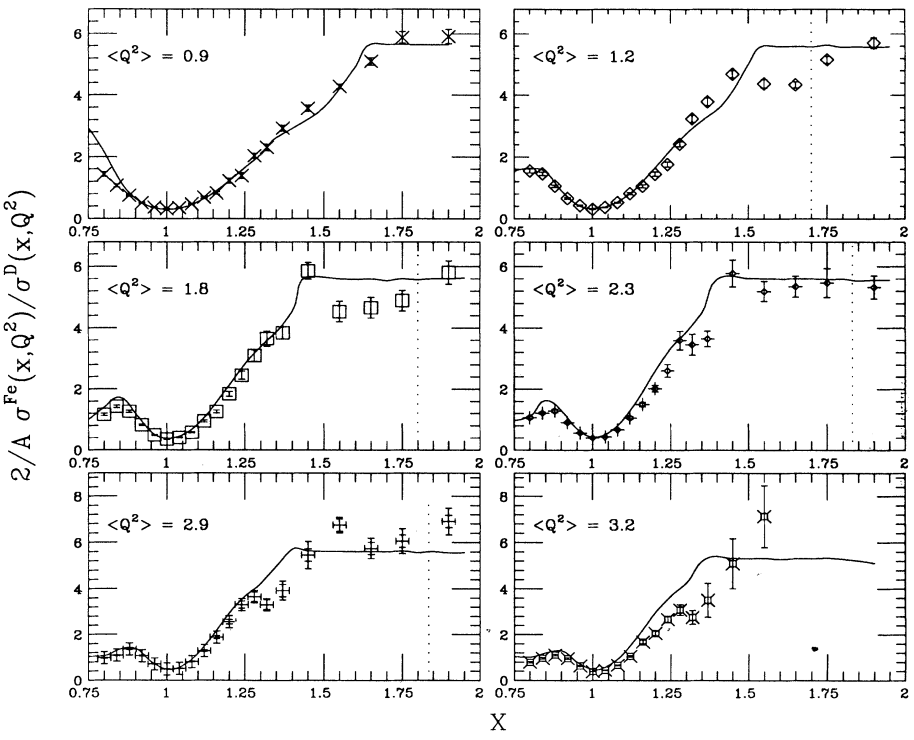

FIG. 3. Ratio $\frac{2}{A}\frac{\sigma_A(x,Q^2)}{\sigma_D(x,Q^2)}$ for ^{56}Fe at six different Q^2's. The average Q^2 is given for each frame. To the right of the vertical dashed line are those data which correspond to a final state less 50 MeV greater than the deuteron rest mass. The solid line is a calculation based on the nuclear spectral function of Ref. [22] (see Sec. VI).

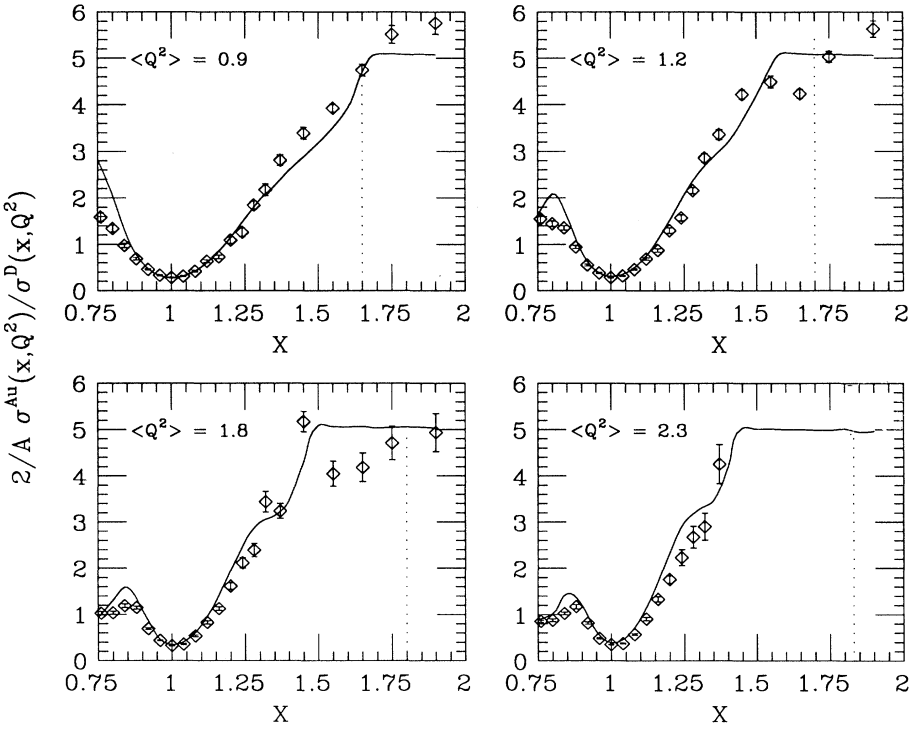

FIG. 4. Ratio $\frac{2}{A}\frac{\sigma_A(x,Q^2)}{\sigma_D(x,Q^2)}$ for ^{197}Au at four different Q^2's. The average Q^2 is given for each frame. To the right of the vertical dashed line are those data which correspond to a final state less 50 MeV greater than the deuteron rest mass. The solid line is a calculation based on the nuclear spectral function of Ref. [22] (see Sec. VI).

of the deuteron with inclusion of the fsi as calculated by Ref. [8] provides a good description of the SLAC deuteron data for $Q^2 \leq 3\text{GeV}/c^2$ [7].

V. LIGHT-CONE PHYSICS AND LIGHT-CONE SCALING

The argument presented above in favor of Eqs. (7) and (8) was implicitly nonrelativistic. But the kinematics under discussion are relativistic, so it is necessary to elaborate. It is well known that the cross sections of hard high-energy processes are expressed through the light-cone (LC) wave functions of nuclei. To see the relevance of LC wave functions, consider the on-shell condition of the struck nucleon,

$$(p^{\text{int}} + q)^2 = m^2 \ , \tag{9}$$

where $p^{\text{int}} = P^A - p^{\text{rec}}$, where p^{rec} is the momentum of the recoiling nucleus. Introducing the LC variables for the virtual photon and the struck nucleon, $q_\pm = q_0 \pm q_3$, for any vector $a_\mu = (a_+, a_-, a_t)$, we have

$$\alpha \equiv \frac{Ap_-^{\text{int}}}{P_-^A}, \ p_t \equiv p_t^{\text{int}} = -p_t^{\text{rec}} \tag{10}$$

and

$$\tilde{m}^2 = \left(P^A - p^{\text{rec}}\right)_+ \left(P^A - p^{\text{rec}}\right)_- - \left(P^A - p^{\text{rec}}\right)_t^2 . \tag{11}$$

Substituting

$$P_+^A = M_A^2/P_-^A,$$

$$p_+^{\text{rec}} = \frac{(m^{\text{rec}})^2 + p_t^2}{(1-\alpha/A)P^+A_-},$$

and

$$\left(P^A - p^{\text{rec}}\right)_- = \frac{\alpha}{A}P_-^A,$$

we obtain

$$\tilde{m}^2 = \left(M_A^2 - \frac{(m^{\text{rec}})^2 + p_t^2}{(A-\alpha)/A}\right)\frac{\alpha}{A} - p_t^2, \tag{12}$$

where m^{rec} is the mass of the recoiling (A–1) nucleus.

Equation (9) can be rewritten as

$$\tilde{m}^2 + q_+p_-^{\text{int}} + q_-p_+^{\text{int}} + q^2$$

$$= \tilde{m}^2 + q_+\frac{M_A}{A}\alpha + q_-\left(\frac{\tilde{m}^2 + p_t^2}{\alpha(M_A/A)}\right) + q^2 = m^2, \tag{13}$$

where at the second step we choose the rest frame of the nucleus $P_+^A = P_-^A = M_A$.

A simple differentiation yields

$$\frac{\partial\alpha}{\partial\tilde{m}^2} = -\left(\frac{1+(q_-/\alpha)(M_A/A)}{(q_+M^A/A)-[q_-(\tilde{m}^2+p_t^2)]/\alpha^2 M_A/A}\right). \tag{14}$$

At sufficiently large Q^2 [several $(\mathrm{GeV}/c)^2$] , q_+ is large enough so that $\frac{\partial\alpha}{\partial\tilde{m}^2}(\tilde{m}^2 - \langle\tilde{m}^2\rangle)$ is rather small. Thus at $Q^2 \sim 2$–3 $(\mathrm{GeV}/c)^2$ α does not depend on (m^{rec}, p_t). Consequently, one can integrate over the recoil mass at fixed α in the expression for the total cross section, which then can be expressed only in terms of α. In formal terms this result means that the cross section is expressed through the light-cone nucleon density matrix [7].

The decrease of $\frac{\partial\alpha}{\partial\tilde{m}^2}$ with increasing Q^2 is not uniform — for $x \geq 1.7 - 1.8$ the decrease is slower. Using Eqs. (12) and (13) it is easy to check that the derivative $\frac{\partial\alpha}{\partial\tilde{m}^2}$ is small for realistic distributions over $\tilde{m}^2$ and for kinematics corresponding to $x < 1.7$, $Q^2 \geq 2$ $(\mathrm{GeV}/c)^2$. As a result

$$\delta\alpha = \alpha(\tilde{m}^2) - \alpha(\langle\tilde{m}^2\rangle) = \frac{\partial\alpha}{\partial\tilde{m}^2}(\tilde{m}^2 - \langle\tilde{m}^2\rangle)$$

and in the essential integration region does not exceed several percent at $Q^2 = 2$ $(\mathrm{GeV}/c)^2$. Thus one can replace the integral over α by taking α at the mean value of $\tilde{m}^2$ in Eq. (14), corresponding to electron scattering from a correlated nucleon pair, where the spectral function has a maximum [10]. Substituting in Eq. (12), $m^{\mathrm{rec}} = m$, $M_A = 2m$, we obtain

$$\langle\tilde{m}^2\rangle \simeq m^2 + 2\alpha_{tn}\left[m^2 - \frac{m^2+p_t^2}{\alpha_{tn}(2-\alpha_{tn})}\right]. \tag{15}$$

Here α_{tn} is the light-cone variable for the interacting nucleon belonging to the correlated nucleon pair. It is determined from the kinematics of the $\gamma^* + (2N) \to N + N$ reaction. The simplest way to calculate α_{tn} is to make use of the invariance of the ratio of the light–cone fractions, p_-^a/p_-^b , under longitudinal boosts. In the c.m. frame of $\gamma^* NN$

$$p_-^{\mathrm{spectN}}/p_-^{\gamma^* NN} = \frac{(E_{0N}+p_{3N})}{2E_{0N}}\bigg|_{\mathrm{c.m.}} = \frac{(1+\sqrt{W^2-4m^2}/W)}{2}. \tag{16}$$

In the rest frame of the two-nucleon pair

$$\alpha_{tn} = 2 - \frac{2p_-^{\mathrm{specN}}}{p_-^{NN}} = 2 - 2\frac{p_-^{\mathrm{spectN}}}{p_-^{\gamma^* NN}}\frac{p_-^{\gamma^* NN}}{p_-^{NN}}. \tag{17}$$

Using $p_-^{\gamma^* NN}/p_-^{NN} = (q_- + 2m)/2m$ we finally obtain

$$\alpha_{tn} = 2 - \frac{q_- + 2m}{2m}\left(1 + \frac{\sqrt{W^2-4m^2}}{W}\right). \tag{18}$$

W is the invariant mass of the two nucleon system ($W^2 = -Q^2 + 4q_0 m + 4m^2$), and $q_- = q_0 - q_3$ is given by Eq. (1). The relation of α_{tn} to x can be seen as a function of Q^2 in Fig. 5.

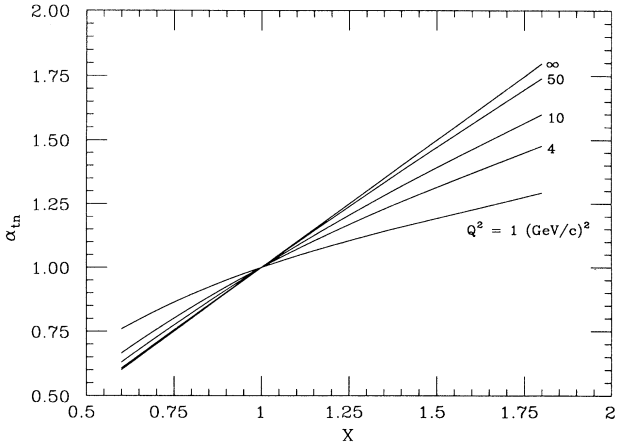

FIG. 5. α_{tn} against x for $Q^2 = 1, 4, 10, 50, \infty$. At $Q^2 = \infty$, $\alpha_{tn} = x$.

The above analysis was based on the consideration of the kinematics of high-energy inclusive electron scattering at large Q^2 and $x > 1$. Thus our conclusion that the cross section depends only on the LC projection of the spectral function holds whatever the formalism used. This property is present implicitly in all approaches used to describe such $A(e,e')$ reactions. However, if the wave function is chosen to be quantized at $t = 0$, as in nonrelativistic quantum mechanics, and not at $t + z =$ constant as in the LC formalism, use of completeness and, hence, the restriction of fsi to nearby neighbors becomes by no means obvious. Thus there is no analog of Eq. (14).

Since cross sections are expressed through the light-cone nucleon density $\rho_A^N(\alpha, p_t)$ at large Q^2 and $x < 2$ this leads to the α_{tn} scaling relation:

$$\frac{\sigma_{A_1}(x,Q^2)}{\sigma_{A_2}(x,Q^2)} = \frac{\int \rho_{A_1}(\alpha_{tn},p_t)d^2p_t}{\int \rho_{A_2}(\alpha_{tn},p_t)d^2p_t}. \tag{19}$$

Thus this ratio of cross sections should be a function of α_{tn} only. Note that the fsi within the SRC are canceled in this ratio to a large extent (cf. the above discussion) and, hence, do not destroy the scaling. We have checked that this relation is satisfied for realistic wave functions both in LC formalism and in the "minimal relativity" formalism of De Forest [17]. This relation is reasonably satisfied by the data, as shown in Fig. 6 where we present σ_A/σ_D as a function of α_{tn} for ^{4}He and ^{56}Fe. Equation (19) will not hold for $Q^2 \geq 6$ $(\mathrm{GeV}/c)^2$ due to the contribution of inelastic processes which lead to an increase of the ratio at fixed α.

The degree of influence of the inelastic channels can be studied. Since the inelastic contributions are not experimentally separated from the elastic contributions in inclusive scattering, a model of the nuclear structure functions is needed. Here we use the model of Ref. [7] [see Eq. (5.28) therein], which is motivated by the physics of color screening effects and is consistent with the EMC (European Muon Collaboration) effect. In Fig. 7 we show a comparison between this model and the data of SLAC experiments [3,5] at $x = 1$. One can

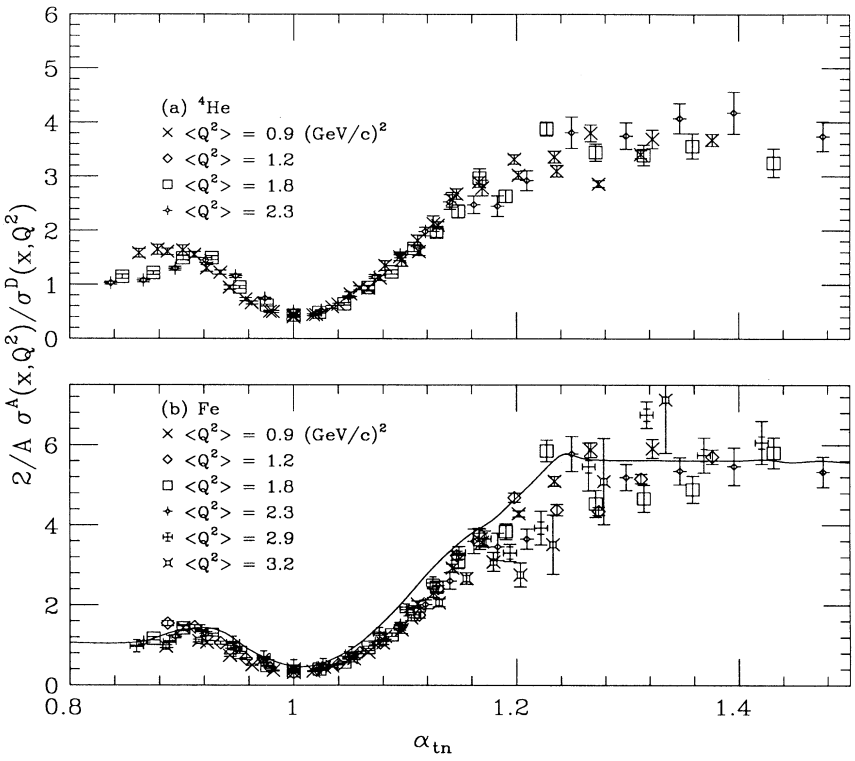

FIG. 6. Ratio $\frac{2}{A}\frac{\sigma_{Fe}(x,Q^2)}{\sigma_D(x,Q^2)}$ for ^{56}Fe for six different Q^2's plotted together against the scaling variable α_{tn}. The solid line is a calculation based on the nuclear spectral function of Ref. [22] (see Sec. VI).

see that in the Q^2 range under discussion the inelastic contribution is small at $x = 1$. For fixed Q^2 its relative importance decreases with increasing x. The saturation of the ratio [Eq. (19)] as seen in Fig. 6 at $\alpha = 1.25 - 1.3$ reflects the dominance of two-nucleon correlations for $k \geq m_N \frac{\alpha-1}{\sqrt{(2-\alpha)\alpha}} \simeq 0.3\,\mathrm{GeV}/c$. Note, however, that the contribution of higher correlations and the motion of the pair in the mean field should lead to a slow increase of the ratio at $\alpha \geq 1.5$; cf. the analysis in [6].

VI. NUMERICAL RESULTS

In principle, calculating the LC density matrix requires a complete relativistic treatment of the problem. However, we are interested in this paper mainly by the kinematical region $\alpha < 2$, where it is sufficient to use a nonrelativistic approximation for the spectral function of the nucleus. In the nonrelativistic approximation the light-cone and nonrelativistic spectral functions must be the same. Formally this statement follows from the form of the master equation for the LC wave function of the nucleus [18]. When non-nucleon degrees of freedom are neglected one finds [7]

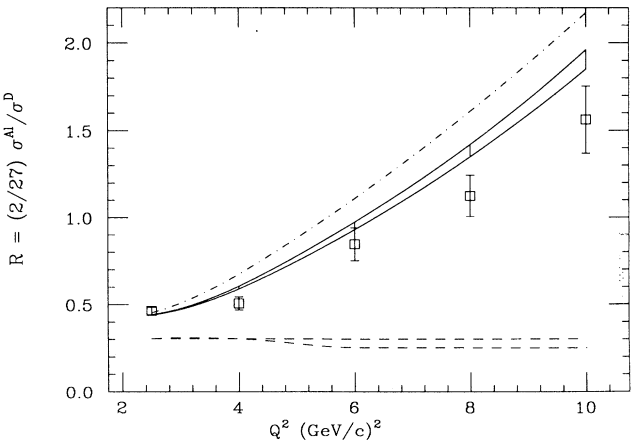

FIG. 7. $\frac{2\sigma^{Al}}{27\sigma^D}$ as a function of Q^2 for $x = 1$. Data is from [5,3]. The dash-dotted curve is a calculation including inelastic channels but without consideration of the EMC effect. The solid curve encloses a range of values that are possible (due to uncertainties in the model) in the color minidelocalization model of the EMC effect [7]. The two dashed curves are the results of a calculation without inelastic contributions with the lower of these including the effect of nucleon swelling.

$$\left.\frac{2\rho_A(\alpha)}{A\rho_D(\alpha)}\right|_{\alpha=1} = \frac{\int n_A(k)(1/k)d^3k}{\int n_D(k)(1/k)d^3k} < 1 \qquad (20)$$

and

$$\left.\frac{2\rho_A(\alpha)}{A\rho_D(\alpha)}\right|_{1.3\le\alpha\le1.7} \simeq a_2(A) \simeq \left.\frac{n_A(k)}{\Psi_D^2(k)}\right|_{k>k_F}, \qquad (21)$$

where $n_A(k)$ is the nonrelativistic momentum distribution of nucleons. The result (21) is obtained by computing the cross section at $\alpha = 1$ and using spherical symmetry to express $n_A(k_t, k_3 = 0)$ in terms of $n_A(k)$.

Equations (20) and (21) both reflect the fact that the nucleus is a more dense system than the deuteron. Equation (20) shows that the deuteron contains more nucleons (per nucleon) with small momenta, $k \ll k_F \sim 270$ MeV/c, than a heavy nucleus. At the same time, heavy nuclei are more dense than the deuteron and therefore have a higher probability of SRC and the probability of high momentum nucleon components increases with nuclear density.

Our treatment is based on using completeness over recoil system states with different $m_{\rm rec}$ at a fixed value of α, which is allowed because $\partial\alpha/\partial\tilde{m}^2$ is small at realistic Q^2. The prescription of [19,20] uses completeness over more restricted phase space corresponding to a fixed four momentum of the struck nucleon. Since momenta of nucleons in SRC are large, $k > k_f$, and corresponding excitations energies E are not small, $\langle E\rangle \sim k^2/2m$, relativistic effects may significantly change Eq. (21), if one tries to calculate $\rho(\alpha, p_t)$ based on the existing calculations of nonrelativistic $S(E, \mathbf{k})$. In the LC quantum mechanics of many-nucleon system [6,7] interacting and spectator nucleons are treated symmetrically, leading to $\rho_A(1+\delta, p_t) \simeq \rho(1-\delta, p_t)$, and small corrections to Eq. (21) both at $\alpha > 1.3$ and $\alpha < 0.7$. In the Bethe-Salpeter-type prescription, used for example in [19,20], the interacting nucleon on average carries less energy than the spectator nucleons (i.e., $m_D - \sqrt{m^2+p^2}$ and $\sqrt{m^2+p^2}$ in the case of scattering off the deuteron). As a result, this formalism leads to $\rho(1+\delta, p_t) < \rho(1-\delta, p_t)$ and this asymmetry is larger for $A > 2$ nuclei than for the deuteron. (For a detailed discussion of this feature of the Bethe-Salpeter models see [21].) As a result, in this formalism one obtains substantially smaller values of the ratio $\rho_A(\alpha)/\rho_D(\alpha)$ at $\alpha \ge 1.3$, approximately by a factor of 1.8–2 as compared to the nonrelativistic results of Eq. (21). Correspondingly, at $\alpha < 0.7$ this formalism leads to significantly larger values of this ratio than Eq. (21).

Information on LC nucleon distributions is also available from the analysis [6,7] of a number of hard nuclear reactions [25], such as fast backward nucleon and pion production, and correlations in $\nu(\bar{\nu}) + A \to \mu^{\pm} + N + X$ reactions where it is found:

$$a_2(^4\mathrm{He}) \simeq 4,\ a_2(\mathrm{C}) \simeq 5-6,\ a_2(\mathrm{Ne}) = 6 \pm 2.$$

Equation (21) combined with calculations [7] of nuclear matter wave functions leads to

$$a_2(A \gg 1) \simeq 5.$$

One can see that these numbers reasonably agree with results of the above analysis of (e, e') data presented here. Note also that the x and α dependences of the ratio of the nucleus and deuteron cross sections is well described (solid line in Figs. 1–4 and 6) in terms of the nuclear spectral function (density matrix), which was taken to be proportional to the deuteron spectral function (density matrix) at $k > k_F$ and Fermi-step-type distribution at smaller k as calculated by Zverev and Saperstein [22]. (For description of the program used in the calculation of the curve in Fig. 3 see [23].) It is worth emphasizing that violation of the "α scaling" (less than 20%) is smaller than the violation seen in y scaling for heavy nuclei at similar momenta [24].

VII. EXTENSION TO COLOR TRANSPARENCY EXPERIMENTS

Let us briefly comment on the utility of this analysis for the color transparency experiments studying $A(p, 2p)$ and $A(e, e'p)$ reactions. One of the problems of these experiments is to convert the experimentally observed cross section of the reaction to the value of the transparency coefficient T with minimal theoretical uncertainty. This problem is especially acute, since theoretical estimates indicate that the color transparency phenomenon would lead to a rather slow increase of T with Q^2. Thus it is necessary to minimize uncertainties due to (a) relatively poor knowledge of the light-cone density matrix for the distribution of nucleons in nuclei, which enters into analysis of high-energy scattering of $A(a, ap)$ reactions (see, e.g. [7]), and (b) possible off-energy-shell effects in the interaction of the projectile with bound nucleons. The idea is that in the impulse approximation the ratio of the cross sections of $A(a, ap)$ and $D(a, ap)$ at fixed α integrated over p_t is equal to the ratio of the light-cone densities, which, as we demonstrated, could be extracted from the ratio of (e, e') cross section with good accuracy. The off-shell effects cancel out in the ratio. Therefore, the transparency can be calculated as

$$T = \frac{\sigma^{A(a,ap)}/\sigma^{D(a,ap)}\,|_{\alpha}}{\sigma^{A(e,e')}/\sigma^{D(e,e')}|_{x(\alpha)}}. \qquad (22)$$

Here $x = \frac{Q^2}{2q_0 m}$ can be calculated through $\alpha = \alpha_{tn}$ using Eq. (18). The α resolution of the experiments does not decrease with increase of the energy, though the resolution in the momentum of the nucleon and in the energy of the recoiling system worsens with increasing Q^2 (for the fixed momentum resolution of spectrometers). Thus $T(\alpha)$ can be measured with better accuracy than $T(k)$.

VIII. CONCLUSIONS

To summarize, we have presented arguments for early dominance of light-cone physics in high Q^2 (e, e') reactions and found supporting experimental evidence for early scaling of the ratios in the light-cone variable. De-

tailed measurements of the discussed ratios would provide a new effective way to study LC nucleon distributions. Such distributions are necessary for many applications, especially for the theoretical analysis of color transparency phenomena. New dedicated measurements of inclusive cross sections as well as $(e, e'p)$, $(e, e'pp)$ reaction with the spectator nucleon flying backward [26] are necessary for detailed investigation of SRC. Such measurements will help us to understand deeper the role of many-nucleon correlations, final state interactions, and the possible role of non-nucleon degrees of freedom.

ACKNOWLEDGMENTS

The authors would like to thank C. Ciofi degli Atti, I. Sick, S. Hepplemann, G. Miller, and S. Liuti for valuable discussions. One of us (M.S.) would like to thank CEBAF for its hospitality while developing codes for (e, e') scattering. This work was supported in part by DOE through Contract Nos. DE-FG05-86ER40262 and DE-FG02-93ER40771.

APPENDIX: fsi OF A STRUCK NUCLEON WITH SLOW NUCLEONS AT $x > 1.3$

Let us consider the problem of the fsi at $x > 1$ in more detail. In the beginning of the paper we explained that for our kinematics the fsi should occur mostly with the other nucleons of the short-range nucleon correlation. Now let us analyze the multiple-scatterine contribution arising when only mean field effects are included in the wave function of the nucleus and all nucleons have low momenta. In this case a nucleon can only acquire high momentum ($\simeq q_3$) by absorbing the virtual photon. (See Fig. 8.) Let us consider how the fast nucleon interacts with the remaining slow nucleons. In this case the struck nucleon has a virtuality

$$\Delta M^2 = m_N^2 - p^2, \tag{A1}$$

where $p = p^{\rm int} + q$. If $|\mathbf{p}^{\rm int}|$ would be small in the kinematics of interest then

$$\Delta M^2 \approx m_N^2 - Q^2\left(-1 + \frac{1}{x}\right) - (p^{\rm int})^2. \tag{A2}$$

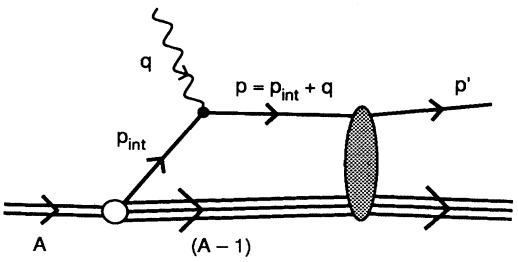

FIG. 8. Reaction diagram for nucleon knockout including final state interactions.

We want to stress that since $\sqrt{\Delta M^2}$ is large it is not legitimate to apply semiclassical approximation for the calculation of the Green function. (We must recall that the semiclassical approximation corresponds to taking the residue over the energy of the fast particle.)

To illustrate the importance of the large virtuality of the struck nucleon let us use the uncertainty principle to estimate mean distances, which are traveled by the struck off–energy–shell nucleon in the nucleus rest frame. We switch here for simplicity to the old fashioned noncovariant formalism where energy is not conserved and momentum is conserved in the intermediate states:

$$r \approx \frac{1}{\Delta E v}, \tag{A3}$$

where v is the struck nucleon velocity, $v = p/E$, and ΔE is given by

$$\Delta E = -q_o - M_A + \sqrt{(m^2 + (q + p^{\rm int})^2} + \sqrt{M_{A-1}^{*2} + (p^{\rm int})^2}. \tag{A4}$$

The results of calculation using Eq. (A3) are presented in Fig. 9 for $x > 1$ for the case where we average over momenta of nucleons with $p < p_{\rm Fermi}$ using the spectral function of [22]. One can see from inspection of Fig. 9 that the struck nucleon can only interact with other nucleons at distances $r \leq 1$ fm, i.e., within the SRC. Note that this estimate is different from the related estimates for deep inelastic scattering. This is because in the quasielastic kinematics $q_0 \ll q_3$, while in deep inelastic processes $q_0 \approx q_3$.

The large virtuality of the interacting nucleon pointed out above leads to the further suppression of fsi, since the rescattering amplitude decreases with the virtuality. In the noncovariant formalism this virtuality is manifested in the large difference of $k_{\rm initial}$ and $k_{\rm final}$ — the absolute values of the momenta of the nucleons before and after the rescattering. They can be written as (neglecting momentum of the second nucleon):

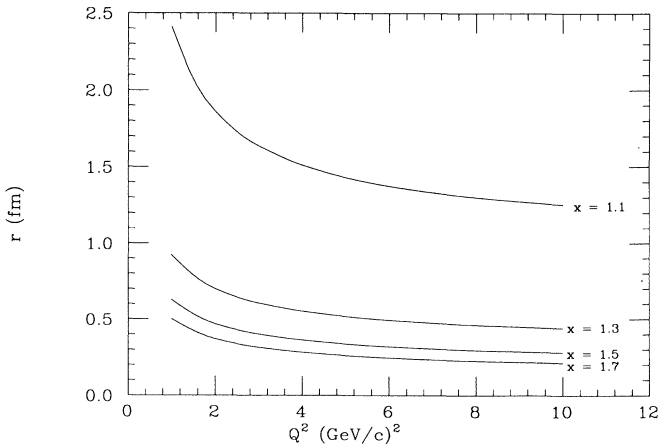

FIG. 9. Maximum distance in Fermi units from the interaction at which fsi can still contribute to the total cross section using Eq. (A3).

$$k_{\rm in} = \{[\sqrt{m^2 + (p_{\rm int} + q)^2} + m]^2 - (p_{\rm int} + q)^2 - 4m^2\}^{1/2}/2, \quad \text{(A5)}$$

$$k_{\rm fin} = \sqrt{(q_0 + m_A - E^*_{A-1} + m)^2 - (p_{\rm int} + q)^2 - 4m^2}/2. \quad \text{(A6)}$$

Here E^*_{A-1} is the energy of recoiling system. For example for $x = 1.5$ and $Q^2 = 2$ GeV/c^2 $k_{\rm in} = 0.65$ GeV/c, while $k_{\rm fin} = 0.41$ GeV/c. (This problem is quite similar to the role of the difference between the masses of the γ and the vector mesons in the photoproduction of vector mesons which leads to lack of nuclear shadowing for nuclear photoabsorption cross section at $E_\gamma \simeq 1 - 3$ GeV. See for example Ref. [27].

The effects discussed in this appendix, which strongly suppress long range fsi in the interaction of virtual photon with slow nucleons of nuclei in the $x > 1$ kinematics, were absent in [20] leading to an overestimate of the fsi. (A similar conclusion has been reached recently in [28].)

[1] S. Rock, R.G. Arnold, P. Bosted, B.T. Chertok, B.A. Mecking, I. Schmidt, Z.M. Szalata, R.C. York, and R. Zdarko, Phys. Rev. Lett. **49**, 1139 (1982).

[2] R.G. Arnold, D. Benton, P. Bosted, L. Clogher, G. DeChambrier, A.T. Katramatou, J. Lambert, A. Lung, G.G. Petratos, A. Rahbar, S.E. Rock, Z.M. Szalata, B. Debebe, M. Frodyma, R.S. Hicks, A. Hotta, G.A. Peterson, R.A. Gearhart, J. Alster, J. Lichtenstadt, F. Dietrich, and K. van Bibber, Phys. Rev. Lett. **61**, 806 (1988).

[3] S. Rock, R.G. Arnold, P.E. Bosted, B.T. Chertok, B.A. Mecking, I. Schmidt, Z.M. Szalata, R.C. York, and R. Zdarko, Phys. Rev. D **46**, 24 (1992).

[4] D. Day, J.S. McCarthy, I. Sick, R.G. Arnold, B.T. Chertok, S. Rock, Z.M. Szalata, F. Martin, B.A. Mecking, and G. Tamas, Phys. Rev. Lett. **43**, 1143 (1979).

[5] D. Day, J.S. McCarthy, Z.E. Meziani, R. Minehart, R. Sealock, S.T. Thornton, J. Jourdan, I. Sick, B.W. Filippone, R.D. McKeown, R.G. Milner, D.H. Potterveld, and Z. Szalata, Phys. Rev. Lett. **59**, 427 (1987); D. H. Potterveld, Ph.D. thesis, California Institute of Technology, 1989.

[6] L.L. Frankfurt and M.I. Strikman, Phys. Rep. **76**, 215 (1981).

[7] L.L. Frankfurt and M.I. Strikman, Phys. Rep. **160**, 235 (1988).

[8] H. Arenhovel, Nucl. Phys. **A384**, 287 (1982); H. Arenhovel and W. Leidemann, Nucl. Phys. **A465**, 573 (1987).

[9] J.G. Zabolitsky and W. Ey, Phys. Lett. B **76**, 1527 (1977).

[10] C. Ciofi degli Atti, L. Frankfurt, S. Simula, and M. Strikman, Phys. Rev. C **44**, R7 (1991).

[11] O. Benhar, A. Fabrocini, and S. Fantoni, Nucl. Phys. **A505**, 267 (1989).

[12] H.J. Pirner and J. Vary, Phys. Rev. Lett. **46**, 1376 (1981).

[13] G. Bertsch, L. Frankfurt, and M. Strikman, Science **259**, 773 (1993).

[14] X. Ji and R. McKeown, Phys. Lett. B **236**, 130 (1990).

[15] W.P. Schütz, R.G. Arnold, B.T. Chertok, E.B. Dally, A. Grigorian, C.L. Jordan, R. Zdarko, F. Martin, and B.A. Mecking, Phys. Rev. Lett. **38**, 259 (1977).

[16] S. Rock, R.G. Arnold, B.T. Chertok, Z.M. Szalata, D. Day, J.S. McCarthy, F. Martin, B.A. Mecking, I. Sick, and G. Tamas, Phys. Rev. C **26**, 1592 (1982).

[17] T. De Forest, Jr., Nucl. Phys. **A392**, 232 (1983).

[18] L.L. Frankfurt and M.I. Strikman, *Modern Topics in Electron Scattering*, edited by B. Frois and I. Sick (World Scientific, Singapore, 1991).

[19] C. Ciofi degli Atti, E. Pace, and G. Salme, Phys. Rev. C **43**, 1155 (1991).

[20] O. Benhar, A. Fabrocini, S. Fantoni, G.A. Miller, V.R. Pandharipande, and I. Sick, Phys. Rev. C **44**, 2328 (1991).

[21] L. Frankfurt, G. Miller, and M. Strikman, Phys. Rev. Lett. **68**, 17 (1992).

[22] M.V. Zverev and Ei.E. Saperstein, Yad. Fiz. **43**, 304 (1986).

[23] M. Sargsyan, CEBAF CLAS Note 90–007 (1990).

[24] D.B. Day, J.S. McCarthy, T.W. Donnelly, and I. Sick, Annu. Rev. Nucl. Part. Sci. **40**, 357 (1990).

[25] E. Matsinos *et al.*, Phys. Zeit. C **44**, 79 (1989).

[26] K.Sh. Egiyan, M.D. Amaryan, G.A. Asryan, R.A Demirchyan, M.S. Ohanjanyan, Yu.G. Sharabyan, S.G. Stepanyan, L.L. Frankfurt, M.I. Strikman, and P.V. Sorokin, Study of Short-Range Properties of Nuclear Matter in Electron-Nucleus and Photon-Nucleus Interactions with Backward Particle Production using the CLAS Detector, CEBAF Proposal PR89-036.

[27] T.H. Bauer, R.D. Spital, D.R. Yennie, and F.M. Pipkin, Rev. Mod. Phys. **50**, 261 (1978).

[28] A.S. Rinat and M.F. Taragin, Weizmann Institute of Science, Report Nos. WIS-91/6/Mar PH, WIS-93/72/Jul PH.